

RESEARCH MEMORANDUM

SOME APPROXIMATE METHODS FOR ESTIMATING THE EFFECTS OF
AEROELASTIC BENDING OF ROCKET-PROPELLED

MODEL-BOOSTER COMBINATIONS

By Richard G. Arbic, George White, and
Warren Gillespie, Jr.

Langley Aeronautical Laboratory
Langley Field, Va.

NATIONAL ADVISORY COMMITTEE
FOR AERONAUTICS
WASHINGTON

March 27, 1953
Declassified February 26, 1958

NATIONAL ADVISORY COMMITTEE FOR AERONAUTICS

RESEARCH MEMORANDUM

SOME APPROXIMATE METHODS FOR ESTIMATING THE EFFECTS OF

AEROELASTIC BENDING OF ROCKET-PROPELLED

MODEL-BOOSTER COMBINATIONS

By Richard G. Arbic, George White, and
Warren Gillespie, Jr.

SUMMARY

Methods are presented for estimating the aeroelastic effects and structural requirements of rocket-propelled model-booster combinations that are nearly symmetrical. Each method is presented according to suitability for a general type of model-booster configuration, each type being covered by one of three cases. The methods differ principally in the manner in which booster stiffness, reference axis, and inertia loading are considered. This analysis permits a computation of the Mach numbers at which either a structural bending divergence or an aerodynamic pitching divergence of the combination may occur for a given flight condition. The increased stiffness, strength, or booster fin size that may be required to minimize aeroelastic effects can be determined.

Flight results are presented for some model-booster combinations flown by the Langley Pilotless Aircraft Research Division. Experience has shown that, when the analysis predicted the combination to be "safe," a successful flight was generally obtained.

INTRODUCTION

Experience in rocket-model testing indicates that the usual method of boosting models (or missiles) to high Mach numbers by mounting the model ahead of a booster generally results in a configuration that is highly susceptible to aerodynamic and structural divergence. Rigid-body methods for determining the strength and static-stability requirements of such aerodynamic bodies are often insufficient for predicting successful flight at high velocity and low altitude. Under these conditions of high dynamic pressure it becomes necessary to consider aeroelastic bending which may cause lift increases and local failure of the structure or

aerodynamic divergence due to forward movement of the center of pressure. Further, bending may progress in such a manner that the lift caused by deformation becomes greater than the lift necessary to produce the deformation so that deflections continue to increase in a divergent manner. This phenomenon is hereinafter called structural divergence.

Methods are presented for estimating the aerodynamic- and structural-divergence Mach numbers of symmetrical or nearly symmetrical model-booster combinations and for determining the structural requirements. Several simplifying assumptions have been made which detract from the accuracy of these methods, but in view of the large saving of time afforded, as compared with a more rigorous dynamic analysis such as that of reference 1, these approximate methods are thought justifiable, especially for preliminary design purposes.

Results obtained by the methods are presented for some model-booster configurations flown at the Langley Pilotless Aircraft Research Station at Wallops Island, Va.

SYMBOLS

a	acceleration, ft/sec ²
α	angle of attack, deg
α_0	applied angle of attack, deg
α_r	resultant angle of attack due to aeroelastic bending, deg
α_{r_w}	resultant angle of attack of wing mean aerodynamic chord (M.A.C.), deg
α_w	angle of attack of model wing necessary to produce zero static stability of the combination, deg
$\Delta\alpha$	initial incremental angle of attack due to bending, deg
$\Delta\alpha_m$	measured incremental angle of attack due to applied load, deg
ϕ	structural angle due to bending, $\alpha_r - \alpha_0$, deg
$\ddot{\theta}$	rotational acceleration, radians/sec ²
$C_{L\alpha}$	lift-curve slope per degree

ϵ	downwash angle, deg
$d\epsilon/d\alpha$	rate of change in downwash angle with angle of attack
I	plane moment of inertia of body cross section, in. ⁴
I_m	mass moment of inertia of model-booster combination in pitch, slug-ft ²
K	initial response factor, $\Delta\alpha/\alpha_0$
E	modulus of elasticity, lb/sq in.
L	lift, lb
L_α	lift per degree angle of attack at maximum design Mach number, lb/deg
m	mass of model-booster combination, slug
M	Mach number
M_a	aerodynamic-divergence Mach number
M_{max}	maximum design Mach number
M_s	structural-divergence Mach number
P	load, lb
P_ϕ	load required to produce 1° of bending deflection, lb/deg
P_0	static pressure, lb/sq ft
q	dynamic pressure, lb/sq ft
S	lifting-surface area, sq ft
X_{cp}	distance from center of pressure to center of gravity of model-booster combination, ft
γ	ratio of specific heats for air

Subscripts:

n	nose
w	wing
b	booster fins

ANALYSIS

General Considerations

Typical model-booster configurations that exhibit divergent and nondivergent tendencies are illustrated in figure 1. For the type possessing a divergent tendency due to aeroelastic bending, lift on the surfaces results in bending of the combination in such a manner as to increase the angle of attack of the forward surface relative to the rear surface, thus tending to destabilize the combination. For the non-divergent model-booster combination, the effect of inertia loads ahead of the forward surface is to reduce the angle of attack of this surface relative to the rear surface and prevent load increases. In this instance, the effect of aeroelastic bending is stabilizing.

Configurations such as those shown in figures 2 to 6 are likely to be of the divergent type. Configurations similar to that in figure 7 may possibly be nondivergent, depending on the mass and its distribution with respect to the area and location of the lifting surfaces. To determine whether such a configuration is subject to aeroelastic divergence requires calculation of the deflection curve for an assumed disturbance, taking into account the effect of inertia loads. If such a configuration as that in figure 7 is of the divergent type, the aeroelastic pitching- and structural-divergence Mach numbers will be relatively high and may not impose a design problem. If of the nondivergent type, a conservative estimate of the strength and static stability of the model-booster combination can be obtained by a rigid-body analysis.

Basic Assumptions

The aeroelastic analysis of the model-booster combination is simplified by the following basic assumptions. The bending response of the combination is assumed to occur very rapidly compared with the pitching response. A simultaneous solution for bending and pitching motions is thereby avoided. The bending response due to a constant 1° applied angle of attack is determined. The amplification of this initial disturbance by aeroelastic bending is sufficient to indicate the effect of aeroelastic bending on the static stability and divergence of the combination. Stationary lift coefficients corresponding to the Mach number range under investigation are used to calculate the incremental air loads that develop during the short time that aeroelastic bending occurs. The additional downwash at the rear surface due to bending of the forward surface is neglected in estimating the air load on the rear surface.

If the flexibility effects of the lifting surfaces of the model and booster are appreciable, their effective lift-curve slopes should be determined by a separate analysis before bending of the combination is analyzed. Although several methods are available for estimating aeroelastic deformation of wings (refs. 2 and 3), the method described in appendix A has been found to give an adequate indication of the effective lift-curve slope of a flexible wing for use in analyzing the bending of the model-booster combination.

The methods presented are most suitable to symmetrical model-booster configurations designed to fly near zero lift. Configurations having several degrees of wing incidence may require further investigation, especially for the estimation of the necessary strength requirements. Some of the problems relating to asymmetrical configurations are discussed under "Results and Discussion" in the section entitled "Special Considerations."

For purposes of further analysis, model-booster configurations are treated under the three cases subsequently described. Although the following cases have been established, not all configurations can be classed by inspection as most suitable to analysis under any particular one of these cases. In general, it may be stated that any configuration can be analysed by the longer method developed for case III.

Case I - Small Model With Large Booster

Configuration.- Case I applies to a configuration consisting of a rigid booster carrying in front of it a small flexible model. The bending deflection of the booster is negligible and the effect of aeroelastic bending of the model and coupling on the static stability of the combination is negligible. Figure 2 shows a configuration of this type. For this case, only a structural-divergence Mach number is determined.

Assumptions.- The following assumptions in addition to the basic ones discussed previously apply to a small model with a large booster:

(1) The contribution of the forward portion (the model) to the static longitudinal stability of the combination is negligible. Load increases on the forward surface due to bending of the sting are not sufficient to destabilize the combination.

(2) Bending stiffness of the rearward portion (the booster) is large compared with that of the forward portion.

(3) The effect of inertia loads is negligible.

(4) The reference flight-path axis is parallel to the booster center line.

Method.- By considering a configuration similar to that shown in figure 2, it can be seen that any aerodynamic disturbance encountered by the forward wing will cause the support sting to bend. This bending will produce an additional angle of attack on the wing which will in turn cause an increase in the air load and further bending of the sting.

An equation can be written to express the convergence (or divergence) of the model structure to an equilibrium angle of attack. This expression is of the form

$$\alpha_r = \alpha_o + \alpha_o \left[\frac{\Delta\alpha}{\alpha_o} + \left(\frac{\Delta\alpha}{\alpha_o}\right)^2 + \left(\frac{\Delta\alpha}{\alpha_o}\right)^3 + \dots + \left(\frac{\Delta\alpha}{\alpha_o}\right)^n \dots \right] \quad (1)$$

where α_r is the equilibrium or resultant angle of attack; α_o , the applied angle of attack; and $\Delta\alpha$, the initial incremental angle of attack due to bending. Letting $\Delta\alpha/\alpha_o = K$ results in the expression

$$\alpha_r = \alpha_o + \alpha_o (K + K^2 + K^3 + \dots + K^n \dots) \quad (2)$$

Substituting $\frac{K}{1-K} = K + K^2 + K^3 + \dots + K^n \dots$ gives

$$\alpha_r = \alpha_o + \alpha_o \left(\frac{K}{1-K} \right) \quad (3)$$

and simplifying yields

$$\frac{\alpha_r}{\alpha_o} = \frac{1}{1-K} \quad (4)$$

Equation (4) applies for $K \leq 1$ and structural divergence occurs for values of $K \geq 1$.

Inasmuch as the aeroelastic behavior of the model structure is linear within the region where $C_{L\alpha}$ is constant, the ratio α_r/α_o , which is the ratio of the equilibrium angle to the applied angle, is essentially an amplification factor that expresses the aeroelastic bending response of the model.

If the sting is sufficiently flexible, the additional air load produced by the bending may be greater than the load from the initial

disturbance ($K \geq 1$), in which case the deflection will continue to increase in a divergent manner until structural failure occurs or until the lift-curve slope is reduced by stalling or other causes. It should be noted that this reasoning applies equally well to wingless bodies such as long pressure probes and various types of "sting" supports, if only the lift derived from the body itself is considered.

The preceding result may also be derived in terms of the loads required for equilibrium. The quantity L_α is used to represent lift per degree angle of attack at maximum-design Mach number on the small forward wing, and $P\phi$, the load required at the center of pressure of this wing to produce 1° bending deflection in the sting.

The lift on the forward wing at any deflected position is then

$$L = L_\alpha(\alpha_0 + \phi) \quad (5)$$

where α_0 is the angle of attack due to the initial disturbance, and ϕ is the angular deflection at the center of pressure caused by bending of the sting.

Elastic restoring load in the sting at any deflected position is merely

$$P = P\phi \quad (6)$$

Since, for equilibrium to be attained, L must be equal to P , the expressions for L and P previously mentioned are set equal and solved for ϕ , so that

$$\phi = \frac{L_\alpha \alpha_0}{P\phi - L_\alpha} \quad (7)$$

It is seen in this equation that if $P\phi$ is equal to or less than L_α , the value of ϕ is either infinitely positive or negative for any value of α_0 , no matter how small. This result indicates a lack of equilibrium, or structural divergence.

Since structural divergence occurs at the Mach number at which $L_\alpha = P\phi$ (or $K = 1$), an expression can be established for the structural-divergence Mach number

$$M_S = \sqrt{\frac{P\phi}{0.7P_0 C_{L_\alpha} S}} \quad (8)$$

where the constant 0.7 equals $\gamma/2$.

Configurations that have a structural-divergence Mach number safely above the anticipated flight range must, nevertheless, be provided with sufficient strength to withstand loads and moments that may be experienced within the flight range. A determination of these loads and moments should consider the amplification of an estimated initial disturbance by aeroelastic bending. For example, if a maximum initial angle of attack α_0 of 0.5° is expected at the critical flight condition, and the amplification factor α_r/α_0 is equal to 3; the configuration should be designed to withstand loads and moments imposed when the forward surface is at $0.5(3) = 1.5^\circ$ and the rearward surface is at 0.5° angle of attack. The normal loads so determined are used in conjunction with estimated longitudinal loads from aerodynamic drag and acceleration. These loads are multiplied by a factor of safety of 1.5 to obtain the design loads. The surfaces should also be checked for flutter. Reference 4 presents flutter criteria which may be used in preliminary design of missile lifting surfaces.

Case II - Large Light Model With Rigid Booster

Configuration.- Figure 3 shows the type of configuration considered suitable to case II. The model is relatively light and flexible compared to the booster and has considerable wing area. Most of the bending results from model and coupling flexibility and this bending has a large effect in reducing the effective static stability of the combination. Mach numbers for both aerodynamic pitching divergence and structural bending divergence are determined.

Assumptions.- The method for case II is based on the following simplifying assumptions in addition to the basic assumptions:

(1) The booster is considered to be a rigid body. Deflection of the combination in flight is due to bending at the model-booster coupling or along the model fuselage, or both.

(2) The center line of the booster is taken as the flight-path axis of the model-booster combination and all angles are referenced to this axis.

(3) The effect of inertia loads is negligible.

Method.- Due to the assumption that the booster is rigid, the model deflects in the same manner as does the sting-mounted model of case I. The method of case I is used to determine the aeroelastic bending of the model and strength requirements of the combination. In addition to providing strength and bending convergence, the combination must also be statically stable aerodynamically at the given Mach number. For the

combination to remain statically stable, it is necessary to insure that the equilibrium angle of attack of the model does not result in sufficient lift to unbalance the stabilizing lift of the booster fins. The angle of attack of the model wing necessary to destabilize the combination can be found by equating the moments of the aerodynamic forces about the combination center of gravity. By considering only the contribution of the model wing and booster fins, the equation is as follows:

$$C_{L_{\alpha_w}} \alpha_w q_w S_w X_{cp_w} = C_{L_{\alpha_b}} \alpha_b q_b S_b X_{cp_b} \left(1 - \frac{d\epsilon}{d\alpha}\right) \quad (9)$$

where the subscript w refers to the model wing and b refers to the booster. By assuming $q_w = q_b$ and $\frac{\alpha_w}{\alpha_b} = \frac{\alpha_w}{\alpha_0}$, the ratio of model-wing angle of attack to the applied angle of attack necessary to reduce the static stability of the combination to zero is

$$\frac{\alpha_w}{\alpha_0} = \frac{C_{L_{\alpha_b}} S_b X_{cp_b} \left(1 - \frac{d\epsilon}{d\alpha}\right)}{C_{L_{\alpha_w}} S_w X_{cp_w}} \quad (10)$$

If, for any Mach number, the ratio α_w/α_0 is greater than α_r/α_0 , the model-booster combination is statically stable. A plot against Mach number of α_r/α_0 and α_w/α_0 will result in two curves; the former being the aeroelastic response of the model and the latter the static stability boundary for the combination. Provided the aeroelastic response curve does not cross the static stability boundary below the maximum Mach number expected, the combination should remain statically stable.

Case III - General Case

Configuration.- The general and most complex case (case III) is that for which bending of the model and booster should be considered because of aerodynamic and inertia loads. Figures 6 and 7 show configurations of this type. The model and booster are of comparable mass and stiffness and the effect of bending on the static stability of the combination may be large. As in case II, Mach numbers for aerodynamic divergence and structural divergence are determined.

Assumption.- The following assumption is peculiar to case III. The longitudinal axis through the center of gravity of the deflected combination about which the radius of gyration is a minimum should be used as a reference line. As an alternative, the more easily determined

line through the centers of pressure of the two largest airloads has been found to be generally satisfactory, depending on a uniform distribution of the configuration mass with respect to the two air loads.

Method.- Air loads are calculated for an angle of attack of 1° and balancing rigid-body inertia loads are determined. On the basis of this loading system, a deflection curve is calculated in the manner explained in appendix B and the reference axis is determined. Deflections of the lifting surfaces with respect to the reference axis are used to calculate additional air and inertia loads. The initial set of loads modified by the additional loads is then applied to the unbent combination to obtain a modified deflection curve and corresponding reference axis. This process is repeated until the bending curve either converges or diverges. If the curve converges, the aerodynamic moment unbalance about the center of gravity is calculated to determine the effective static stability. The moment unbalance is calculated at different Mach numbers and plotted to determine the Mach number for which the moment is zero. Aerodynamic pitching divergence of the combination is assumed to occur at this Mach number.

The foregoing procedure may be shortened if the initial deflections of lifting surfaces obtained from the first bending curve are converged separately without calculation of additional bending curves, and the

unbalanced moment is then calculated. The equation $\frac{\alpha_r}{\alpha_0} = \frac{1}{1 - K}$ may be

used in the manner described previously when the initial deflection of the surface is in the direction to increase the air load. The equation

$\frac{\alpha_r}{\alpha_0} = \frac{1}{1 + K}$ should be used when the air load is reduced. For the first

condition a Mach number for structural divergence is determined when K is equal to 1. If the lift-curve slopes and center-of-pressure locations are assumed to be constant over the Mach number range of interest, initial deflections of the lifting surfaces at any Mach number can be calculated from those at a given Mach number by making use of the fact that initial deflections and air loads vary directly with the square of the Mach number. These sets of deflections are then converged.

If a one-step solution is desired, the initial incremental angles of attack $\Delta\alpha$ of the various lifting surfaces are calculated at M_{\max} for $\alpha_0 = 1^\circ$. These values are inserted in the following equation which is then solved for the aerodynamic-divergence Mach number M_a :

$$L_{\alpha_n} X_{cpn} \left(\alpha_0 + \Delta\alpha_n \frac{M_a^2}{M_{max}^2} \right) + L_{\alpha_w} X_{cpw} \left(\alpha_0 + \Delta\alpha_w \frac{M_a^2}{M_{max}^2} \right) + L_{\alpha_b} X_{cpb} \left(\alpha_0 + \Delta\alpha_b \frac{M_a^2}{M_{max}^2} \right) = 0 \quad (11)$$

A design criterion for strength similar to that used for case I and case II configurations may be used on case III configurations. Since the resultant equilibrium angle of attack at the rear surface obtained by the method of case III may be less than the initial applied angle of attack, the design of the rear portion of the configuration by the set of resultant equilibrium deflections would be optimistic. To avoid such optimism, the configuration should be checked separately for both the initial applied disturbance and the final equilibrium conditions.

MODELS AND TESTS

Typical model-booster combinations flown by the Langley Pilotless Aircraft Research Division (at its testing station at Wallops Island, Va.) are shown in figures 2 to 7. The combinations were either of all metal or metal and wood construction with the model in nearly all cases free to separate from the booster after booster-motor burnout. The models were generally instrumented with a telemeter that transmitted, among other quantities, the normal acceleration at the model center of gravity. The burning time of the different solid-fuel-booster rocket motors varied between 1 and 3 seconds. During the boost period the model-booster combinations were subject to possible aeroelastic bending effects.

The aeroelastic-divergence Mach numbers were calculated for these model-booster combinations by the methods presented previously. For use in the analysis by the method of case II, static-deflection tests were made of the model and its booster coupling to determine their flexibility. A typical test setup is shown in figure 8. For models of the type shown in figure 4, the flexibility of the wing was simultaneously investigated by applying the test load at the 40-percent M.A.C. location of each wing panel. Dial gages were located to measure the rotation of the wing M.A.C. and deflection along the body. An initial load was applied to take up looseness of the model in the coupling, insuring that linear deflections would be obtained. Table I lists additional models

of the type shown in figures 3 and 4. Some of these models and booster couplings incorporated modifications which reduced the deflections found by the initial static tests of the configuration.

RESULTS AND DISCUSSION

Cases I and II were set up in an effort to reduce the amount of computation required by the general analysis for case III. Further, the methods of cases I and II are well-suited to a simple static test of the actual model and coupling before flight. Such a test may indicate loose rivet joints or other additional sources of deflection not apparent in the preliminary design. It will not always be possible, however, to classify by inspection a new configuration as most suitable to analysis by any particular one of these cases. If the rigidity of the booster is in doubt or if the mass of the model is sufficient to warrant consideration, the method of case III should be used.

Case II - Large Light Model With Rigid Booster

Data in figures 9 to 12 pertain to the arrow- and sweptback-wing configurations of figures 3 and 4, respectively. For the application of the method of case II, the static-deflection test data were plotted as shown in figure 9 and the angles of the body and wing M.A.C. were determined for the applied load. The arrow wing was assumed rigid and the angle of the body and wing are, therefore, seen to be the same. For the more flexible swept-wing model, the angle of the wing M.A.C. is less than the angle of the body (or of a rigid wing). The modified booster couplings are seen to result in less severe bending, especially for the arrow-wing configuration.

The curves of figure 10 were obtained from an estimate of the rigid-wing lift per degree angle of attack used in conjunction with the measured incremental angles shown in figure 9 for the wing and body. The initial incremental angles $\Delta\alpha$ due to an applied angle of attack α_0 were determined as follows for the various Mach numbers:

$$\frac{\Delta\alpha}{\alpha_0} = \Delta\alpha_m \frac{\text{Lift per degree}}{\text{Applied load}}$$

where $\Delta\alpha_m$ is the measured angle due to the applied load. Values of $K = \Delta\alpha/\alpha_0$ were then plotted against Mach number. Values of $K \geq 1$ are seen to result in structural divergence. In figure 10(a) the point shown, based on calculated stiffness for model 1, illustrates the

improvement over models 2, 3, and 4A as a result of the use of a solid- rather than a hollow-steel tail cone for "mating" with the booster coupling. In figure 10(b) the two upper curves are the initial responses for the body with original and modified coupling and, thus, represent the rigid-wing responses. The two lower curves are the initial responses for the steel and 75S-T6 aluminum-alloy wing on the body with modified coupling and, thus, show the improvement due to wing flexibility.

The aeroelastic-bending-response curves of figure 11 were obtained by substituting values of K from figure 10 in the previously derived equation $\frac{\alpha_r}{\alpha_0} = \frac{1}{1 - K}$. The static-stability boundaries were obtained by equation (10). Separate stability boundaries were obtained in figure 11(b) for a rigid wing and for a solid 75S-T6 aluminum-alloy wing by using appropriate values of rigid and flexible wing lift-curve slope. The effective wing lift-curve slope for the 75S-T6 wing was obtained by the method outlined in appendix A.

Figure 11 shows that the intersection of the aeroelastic response curve and the static-stability boundary occurs at a lower Mach number than does the structural-divergence Mach number. In fact, the data of this figure indicate that infinite static stability would be necessary in order for failure to occur because of structural divergence. Further, excepting very slight disturbances, deflections would probably result in a local failure of some part of the structure before structural divergence could occur. For model-booster combinations of this type, therefore, the structural-divergence Mach number is probably not a safe criterion for predicting failure. For small sting-mounted models on a highly stable booster which approach the models of case I, however, the structural- and aerodynamic-divergence Mach numbers would not be so widely different and prediction of failure on the basis of structural divergence would not be too unconservative provided strength requirements were met. This can be visualized from figure 11(a) by imagining the static-stability boundary displaced upward and by noticing that the intersection of this boundary with the solid-line bending-response curve (for models 2, 3, and 4A) approaches the Mach number for structural divergence.

The most effective means of increasing the structural- and aerodynamic-divergence Mach numbers is by stiffening the model-booster combination, but for a given aeroelastic-bending-response curve (or for a given stiffness), the aerodynamic-divergence Mach number can also be increased by providing the combination with larger and more effective booster fins. In figure 11(b), wing flexibility is seen to result in less severe aeroelastic bending and in more effective static stability.

Models 2 and 3 in figure 11(a) failed at a higher Mach number than that shown for aerodynamic divergence. One explanation for this result lies in the fact that aerodynamic divergence does not necessarily result in immediate failure of the structure. Since figure 11 applies regardless of the magnitude of the disturbance, it is evident that, for a slight disturbance, the loads encountered when aerodynamic divergence occurs might not be sufficient to cause structural failure, but that failure would occur soon afterwards due to rapidly increasing loads. The curve of normal accelerations for model 3 in figure 12 appears to substantiate this reasoning because of the rapid increase in normal accelerations just before failure. It is of interest to note that aerodynamic divergence appears to have begun at approximately 1.3 seconds corresponding to a Mach number of about 0.9 and that near aerodynamic instability is predicted in this Mach number region in figure 11(a) for model 3. Unfortunately, model 2 did not carry a normal accelerometer and the aforementioned evidence of aerodynamic divergence was, therefore, not supported by this model. Model 3 is believed to have failed at a lower Mach number than did model 2 because it had deflected ailerons forcing the combination to roll and, thus, producing additional stresses. A second explanation of the apparent discrepancy between the Mach number predicted for aerodynamic divergence and the actual failure Mach number is that the method is conservative. This fact is borne out by the calculated point for model 1 which predicts aerodynamic divergence, whereas the combination actually experienced a successful boost. Not all of this apparent discrepancy for model 1 is attributed to conservatism of the method, however, for it is thought that some unknown factors contributed to the success of the model-booster combination and that repeated flights would not necessarily have been successful. For example, examination of figure 12, which shows velocity and normal acceleration during boost, reveals that the arrow-wing combination was subject to an abrupt transonic trim change. This trim change is seen to occur at approximately the same velocity for the combinations of models 1 and 4c. The ability of the combination to negotiate this trim change, coupled with the long period of the nearly statically unstable combination, could possibly have played a part in the success of model 1, for it is evident that the combination had a tendency to trim to negative normal force and the sudden transonic trim change resulted in positive normal force permitting the combination to start trimming anew to negative normal force. The model-booster combinations of models 5B, 6, and 7 are seen to have experienced no sudden transonic trim changes, but merely trimmed slowly to negative normal force.

Case III - General Case

In figure 13 is shown the deflection curve at Mach number 0.9 and a plot of unbalanced moment against Mach number for the model-booster combination of figure 5. The deflection curve was calculated by the

method of appendix B, and, for calculation of unbalanced moment, it was assumed that deflections at Mach numbers other than 0.9 were a function only of dynamic pressure, the aerodynamic derivatives remaining constant. Figure 13(b) shows that for this configuration the converged solution by the general method (case III) gives results which are more conservative than a one-step solution by the same method. Results by the method of case II are included for comparison and show more conservative results than the converged solution by the general method for this combination.

Tabular results are presented in table II for the configurations of figures 3 to 7. This table gives the calculated aerodynamic-divergence Mach number obtained by the methods of either case II or case III (one-step solutions) or of both methods where available and also gives the maximum-flight Mach number attained by the combination at separation or failure. The results for the configuration of figure 7 were included to show that a combination of this type has a relatively high aerodynamic-divergence Mach number largely because of the rearward location of the model wing.

Special Considerations

The methods herein presented have been used with satisfactory results for predicting the capabilities of symmetrical and slightly asymmetrical model-booster combinations, but some difficulty has been encountered with configurations having a considerable degree of asymmetry. For example, some airplane-type configurations require the use of a "shovel type" booster coupling similar to the modified coupling shown for the arrow-wing configuration. Such a coupling must not interfere with drag-inertia separation of the model at booster burnout, and care must be taken in the design to insure that the vertical center of gravity of the combination is not displaced too far from the thrust center line. Attempts to keep the vertical center of gravity of the combination on the center line by designing booster fins whose mass would balance the forward off-center-line mass have not proved very successful since high local bending moments result from the mass offset and thrust acceleration, in some cases contributing additional destabilizing bending deflections.

Some airplane-type configurations have been found to experience very high normal accelerations during boost through the transonic speed range. This apparent "trim change" has sometimes resulted in structural failure of the model-booster combination. Such a trim change for the arrow-wing configuration can be seen by examination of the normal acceleration curves in figure 12. For this configuration, however, the normal accelerations experienced were not very high. Since the model-booster combinations are usually designed with a small margin of safety on strength, any unforeseen increase in trim angle of attack is likely to cause structural failure. This problem is complicated somewhat by the uncertainty in prediction of the trim angle for previously untested configurations.

As a result of the foregoing considerations, asymmetrical configurations have been found to require a more extensive analysis than is provided by the methods herein presented. Since, for these configurations, failure is not necessarily a result of aeroelastic divergence, a larger safety factor on strength has been found desirable in order to prevent structural failure due to unforeseen transonic trim changes and other possible effects of asymmetry.

The methods presented herein are based on an assumed instantaneous disturbance and further assume that the aeroelastic bending response of the combination is more rapid than the aerodynamic pitching response, so that the combination does not have time to rotate into the relative wind because of its inherent static stability. In many cases, the largest normal force instigating aeroelastic bending is a result of model-wing misalignment relative to the booster fins (arising from construction tolerances or wing incidence) rather than a sudden disturbance such as a gust. The normal forces due to misalignment are present from the start of booster flight and increase with Mach number permitting the combination to bend and trim to an equilibrium angle of attack. Thus, the model-booster combination can experience either sudden disturbances due to gusts or a gradual disturbance due to misalignment, or both. The methods presented are assumed valid for any of these conditions provided the misalignment between the major lifting surfaces is small so that the surfaces of the unbent combination experience essentially the same angles of attack. For combinations having forward and rearward surfaces set at different angles of incidence, the bending response of the combination should be based on the estimated angle of attack of the different surfaces when the unbent combination is trimmed in flight, since the elastic curve thus obtained would probably be somewhat different from that obtained by assuming equal applied angles of attack for each surface. Except for the use of these different initial applied angles, the method of obtaining the aerodynamic divergence Mach number is the same as that presented for case III by either a one-step calculation of the combination deflection curve or by the complete convergence process. For calculation of strength requirements, the converged solution for the equilibrium angle of attack of the forward portion should always be used since this procedure produces a more severe loading condition. The rearward portion, however, experiences a greater angle of attack when the combination is unbent, and, therefore, should be designed to withstand the maximum angle of attack estimated for the unbent condition. Further, it is possible that a gust will strike the combination when it is already bent because of wing incidence, thus producing additional loading. A factor of safety should, therefore, be included in the strength calculations to account for this and other unknown conditions.

In some instances, it may be important to consider the effect of booster-thrust misalignment as a result of bending of the combination. Examination of the deflection curves in figures 13 and 14 reveals that

the effect of bending is to produce destabilizing moments due to thrust misalignment with respect to the center of gravity of the combination. For combinations having considerable flexibility, these moments may reach significant magnitudes.

Accuracy

The accuracy of the methods presented herein is largely dependent upon the assumptions and the applicability of the assumptions to the configuration. Since no comprehensive program has been conducted to investigate the problem of aeroelastic divergence or to verify the assumptions, the degree of accuracy can be based only on the results obtained with the various methods.

The one-step solution for the general method (case III) has been most widely used and has, in general, proved sufficient. The complete solution is recommended, however, since it is believed to result in a more accurate estimate of the aeroelastic-divergence Mach numbers.

The method of case II has been used only recently, and, therefore, even less is known of the accuracy afforded by this method. However, for the configurations investigated by this method, there has been no evidence of aeroelastic divergence when the combination was found "safe" or "marginal." The only combinations found "unsafe" by this method were those of models 1 to 3 reported herein and they attained a higher Mach number than that predicted for static instability. Thus, on the basis of the results available to date, the method of case II is thought to give a conservative estimate of the aerodynamic- and structural-divergence Mach numbers.

CONCLUSIONS

The results presented of the effects of aeroelastic bending of model-booster combinations indicate the following conclusions.

1. Failure to consider the effect of aeroelastic bending will usually result in an unconservative estimate of the structural strength requirements and static stability of model-booster combinations.

2. Aerodynamic divergence due to static instability generally occurs at a lower Mach number than does structural divergence.

3. The aerodynamic-divergence Mach number can be increased by increasing the bending stiffness of the model-booster combination or by increasing the size and effectiveness of the booster fins.

Langley Aeronautical Laboratory,
National Advisory Committee for Aeronautics,
Langley Field, Va.

APPENDIX A

APPROXIMATE DETERMINATION OF EFFECTIVE LIFT-CURVE SLOPE

If the aerodynamic lifting surfaces of the model-booster combination are subject to large aeroelastic effects, their effective lift-curve slopes should be determined and these values used in the calculation of aeroelastic bending of the combination. For example, if a rigid-wing analysis shows marginal static stability or instability of the combination, for the case of a model with a sweptback flexible wing, an analysis considering the reduced effective lift-curve slope of the model wing may show no danger of static instability. This result is due to the fact that flexibility of a sweptback wing results in less severe loading on the wing and, therefore, less severe aeroelastic bending of the combination and lower destabilizing moments due to model bending. Conversely, a rigid-wing analysis for a straight or swept-forward flexible wing may be unconservative.

The following approximate method may give a satisfactory indication of the wing-flexibility effects on the aeroelastic bending response and static-stability boundary of the combination. This method utilizes data from a static-deflection test of the lifting surface and is based on the assumption that the rotation of the M.A.C. due to a point load applied at the center-of-pressure location on the M.A.C., is indicative of the flexibility of the surface.

For a flexible sweptback wing, the convergence of the wing M.A.C. to an equilibrium angle of attack can be expressed as follows:

$$\alpha_{r_w} = \alpha_0 - \alpha_0 \left[\frac{\Delta\alpha_w}{\alpha_0} - \left(\frac{\Delta\alpha_w}{\alpha_0} \right)^2 + \left(\frac{\Delta\alpha_w}{\alpha_0} \right)^3 - \left(\frac{\Delta\alpha_w}{\alpha_0} \right)^4 \dots + \left(\frac{\Delta\alpha_w}{\alpha_0} \right)^{n-1} - \left(\frac{\Delta\alpha_w}{\alpha_0} \right)^n \dots \right] \quad (12)$$

where α_{r_w} is the resultant or equilibrium angle of attack of the wing M.A.C.; α_0 , the applied angle of attack; and $\Delta\alpha_w$, the initial incremental twist of the wing M.A.C. with respect to the model center

line. Letting $K = \Delta\alpha_w/\alpha_0$ and substituting $\frac{K}{1+K} = K - K^2 + K^3 - K^4 + \dots + K^{n-1} - K^n + \dots$ gives

$$\frac{\alpha_{r_w}}{\alpha_0} = \frac{1}{1+K} \quad (13)$$

The ratio α_{r_w}/α_0 in equation (13) is the ratio of flexible- to rigid-wing lift-curve slope. Thus,

$$C_{L\alpha_{flexible}} = \frac{\alpha_{r_w}}{\alpha_0} C_{L\alpha_{rigid}}$$

A similar analysis for straight and sweptforward wings would result in an equation identical to equation (4), since, for these wings, the equilibrium angle would be greater than the applied angle; whereas, for the sweptback wing, the equilibrium angle is less than the applied angle.

APPENDIX B

METHOD OF OBTAINING DEFLECTION CURVE OF THE MODEL-BOOSTER

COMBINATION FOR THE GENERAL CASE

Figure 14 indicates the steps in obtaining the deflection curve of model-booster combination for application of the method of the general case. The procedure illustrated is easily adaptable to tabular form and the computation is generally performed in this manner. The example presented is for calculation of deflections in the XZ-plane, that is, calculation of deflections that would affect the longitudinal stability of the combination.

Calculation of the deflection curve is reduced to a problem in statics by considering an equilibrium force system consisting of applied lift forces resisted by rigid-body inertia forces equal in magnitude but opposite in direction to the lift forces. The first step consists of dividing the combination into incremental lengths convenient to the calculation of the weight distribution. Once the weight distribution has been determined, the rotational and translational inertia load factors due to an assumed unit angle of attack are determined and are added to obtain the total load factor. The load factor is the acceleration in g at any station along the combination and is obtained from the basic relations $L = ma$ and $LX_{cp} = I_m \ddot{\theta}$. The product of the ordinates of the weight-distribution curve and the total load factor gives the inertia load distribution. Double integration of the load-distribution curve with consideration of applied lift loads results in determination of the bending-moment curve. From the moment curve and the known stiffness (EI) distribution, a curve of Moment/EI is plotted. Double integration of this Moment/EI curve then produces the deflection curve. From the deflection curve, the incremental angles of attack of the model and booster lifting surfaces are measured with respect to the assumed zero reference line and are converged (for the complete solution) or combined with the originally assumed unit angle of attack (for one-step solution) to determine unbalanced moment as described in the text.

REFERENCES

1. Dylke, E. R., Goerke, R. F., and Daughaday, H.: Structural Design Criteria for Boosted Flight of the MBV-3a. Rep. No. BAC-22, Bell Aircraft Corp., Dec. 1, 1948.
2. Diederich, Franklin W., and Foss, Kenneth A.: Charts and Approximate Formulas for the Estimation of Aeroelastic Effects on the Loading of Swept and Unswept Wings. NACA TN 2608, 1952.
3. Skoog, Richard B., and Brown, Harvey H.: A Method for the Determination of the Spanwise Load Distribution of a Flexible Swept Wing at Subsonic Speeds. NACA TN 2222, 1951.
4. Martin, Dennis J.: Summary of Flutter Experiences As a Guide to the Preliminary Design of Lifting Surfaces on Missiles. NACA RM L51J30, 1951.

TABLE I
 MODELS OF THE ARROW- AND SWEEP-WING CONFIGURATIONS
 OF FIGURES 3 AND 4

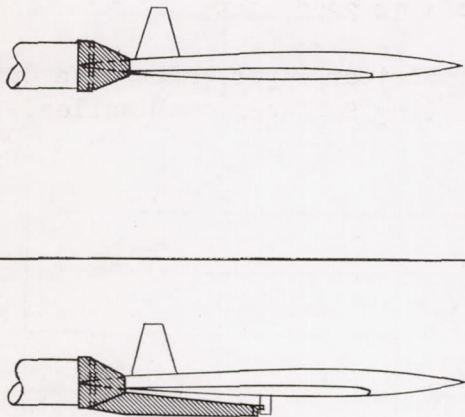
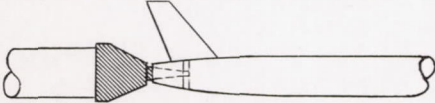
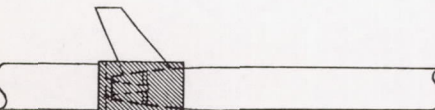
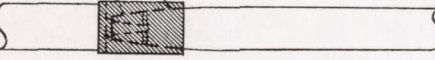
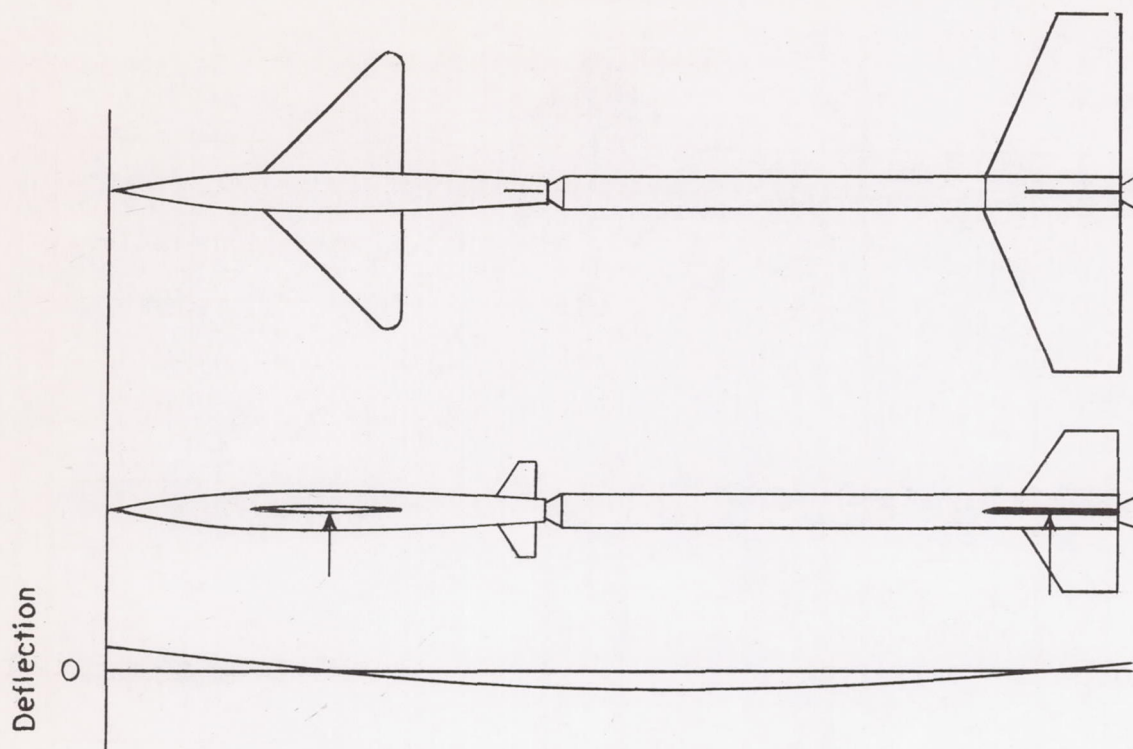
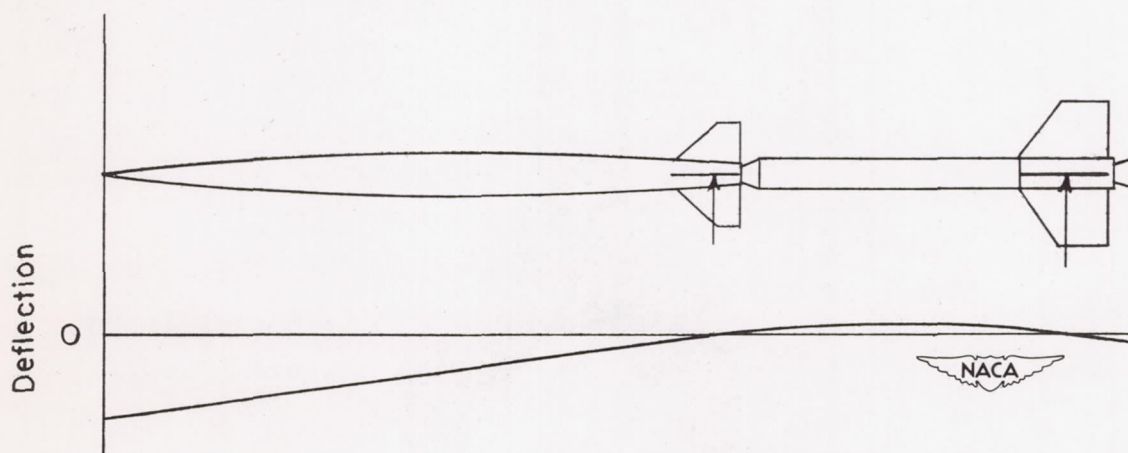
Model number	Type of model-booster coupling	Remarks
Arrow-wing configuration		
1		Drag model. No deflected controls. Solid-steel sting for mating with booster coupling. Successfully boosted.
2		Drag model. No deflected controls. Hollow-steel sting. Unsuccessfully boosted.
3		Roll model with elevons deflected $2\frac{1}{2}^{\circ}$. Hollow-steel sting. Unsuccessfully boosted.
4A		Same as model 2. Model not flown in this condition.
4B		Model 4A with modified type booster coupling. Not flown in this condition.
4C	Model 4A with modified type coupling and internal reinforcement to body center section. Successfully boosted.	
Swept-wing configuration		
5A		Drag model. No deflected controls. Not flown with original type of coupling. 75S-T6 aluminum-alloy wing.
5B		Model 5A with modified type of booster coupling. Successfully boosted.
6		Same as model 5B. Successfully boosted.
7		Same as models 5B and 6 but with steel wing. Successfully boosted.

TABLE II
SUMMARY OF RESULTS

Model number	Model-booster configuration	Calculated M_a		M, at separation	M, at failure
	Figure	Case II	Case III, one-step		
1	3		1.35	1.97	
2		1.03	1.28		1.42
3		1.03	1.28		1.18
4C		Above 2.0		1.58	
5B	4	Above 1.5		1.36	
6		Above 1.5		1.43	
7		Above 1.5		1.30	
8	5	0.9	1.22	0.9	
9	6		2.1	1.9	
10	7		6.5	2.1	



(a) Divergent.



(b) Nondivergent.

Figure 1.- Typical divergent and nondivergent type of configurations and deflection curves.

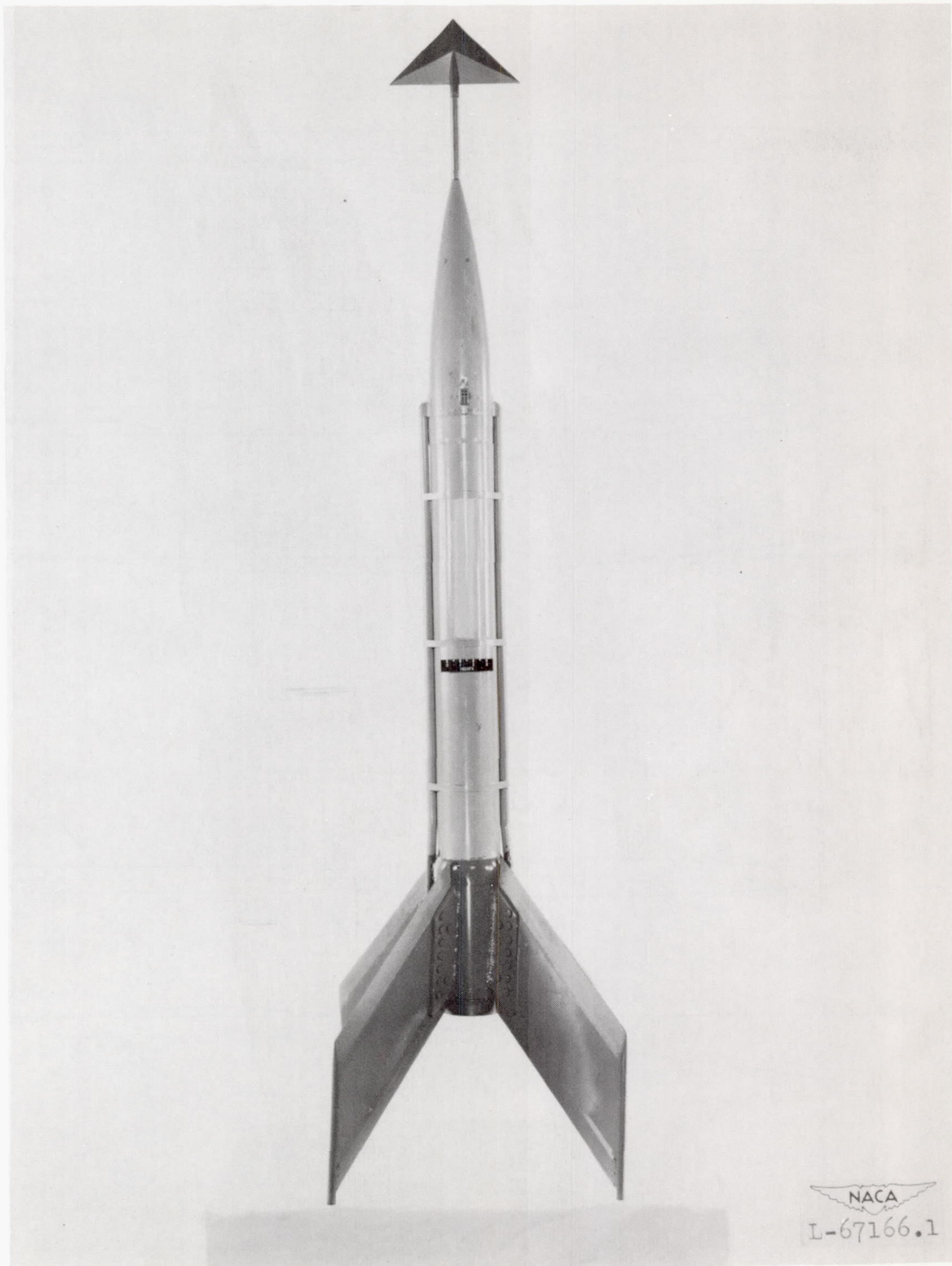


Figure 2.- Sting-mounted model and booster.

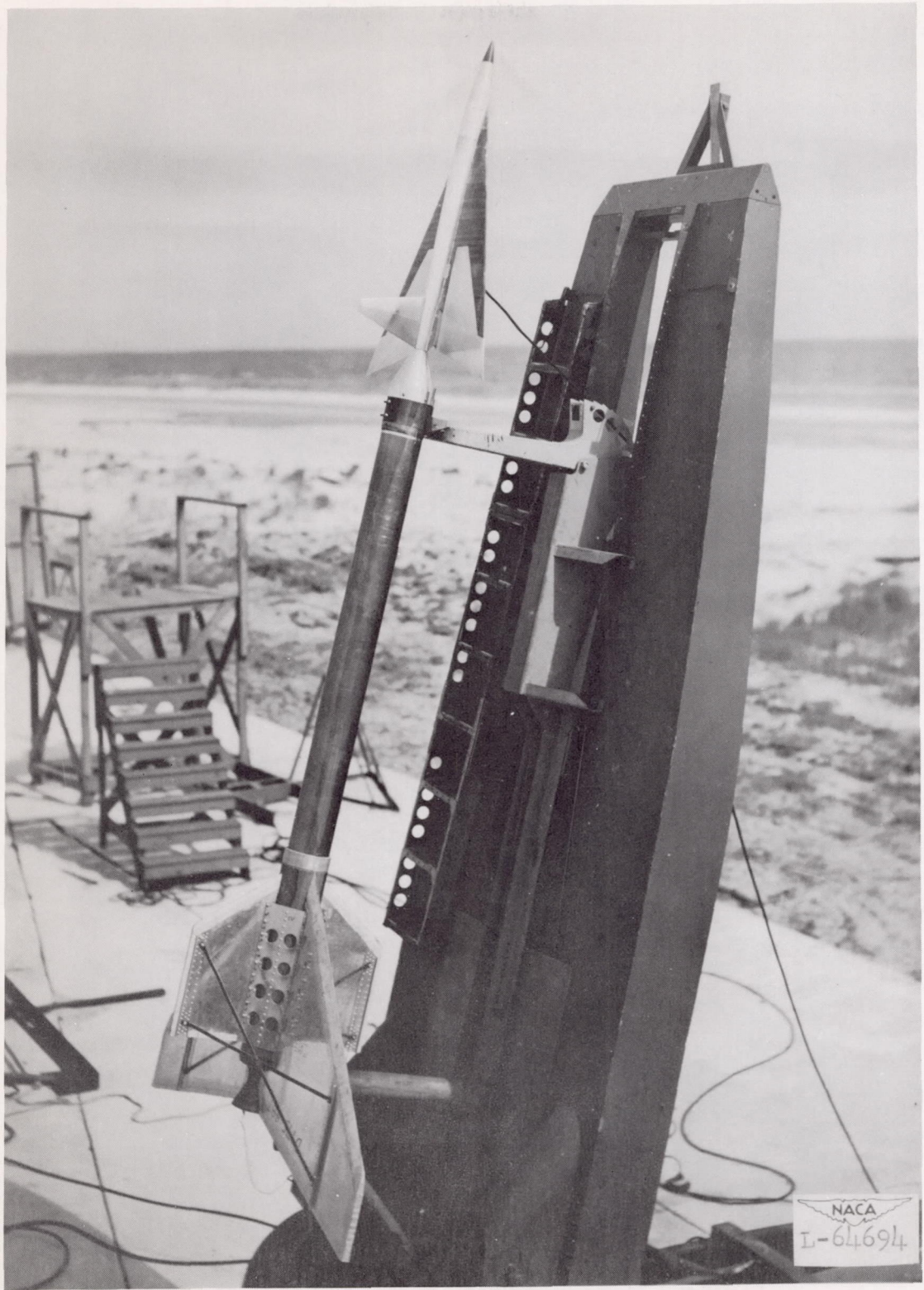


Figure 3.- Arrow-wing drag model and booster.



Figure 4.- Sweptback-wing drag model and booster.



Figure 5.- Sweptback-wing buffet model and booster.



Figure 6.- Cruciform missile model and booster.

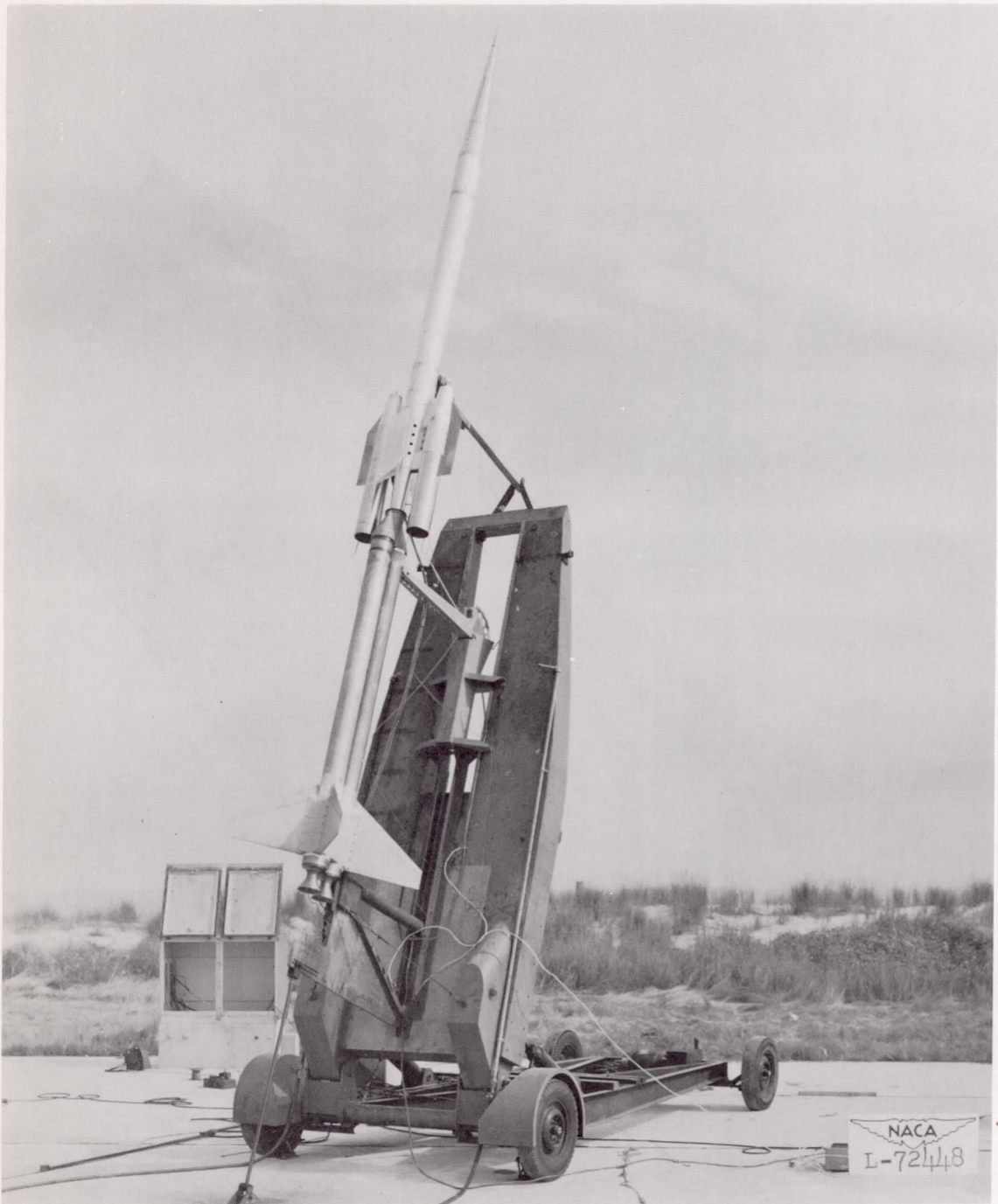


Figure 7.- Ram-jet model and booster.

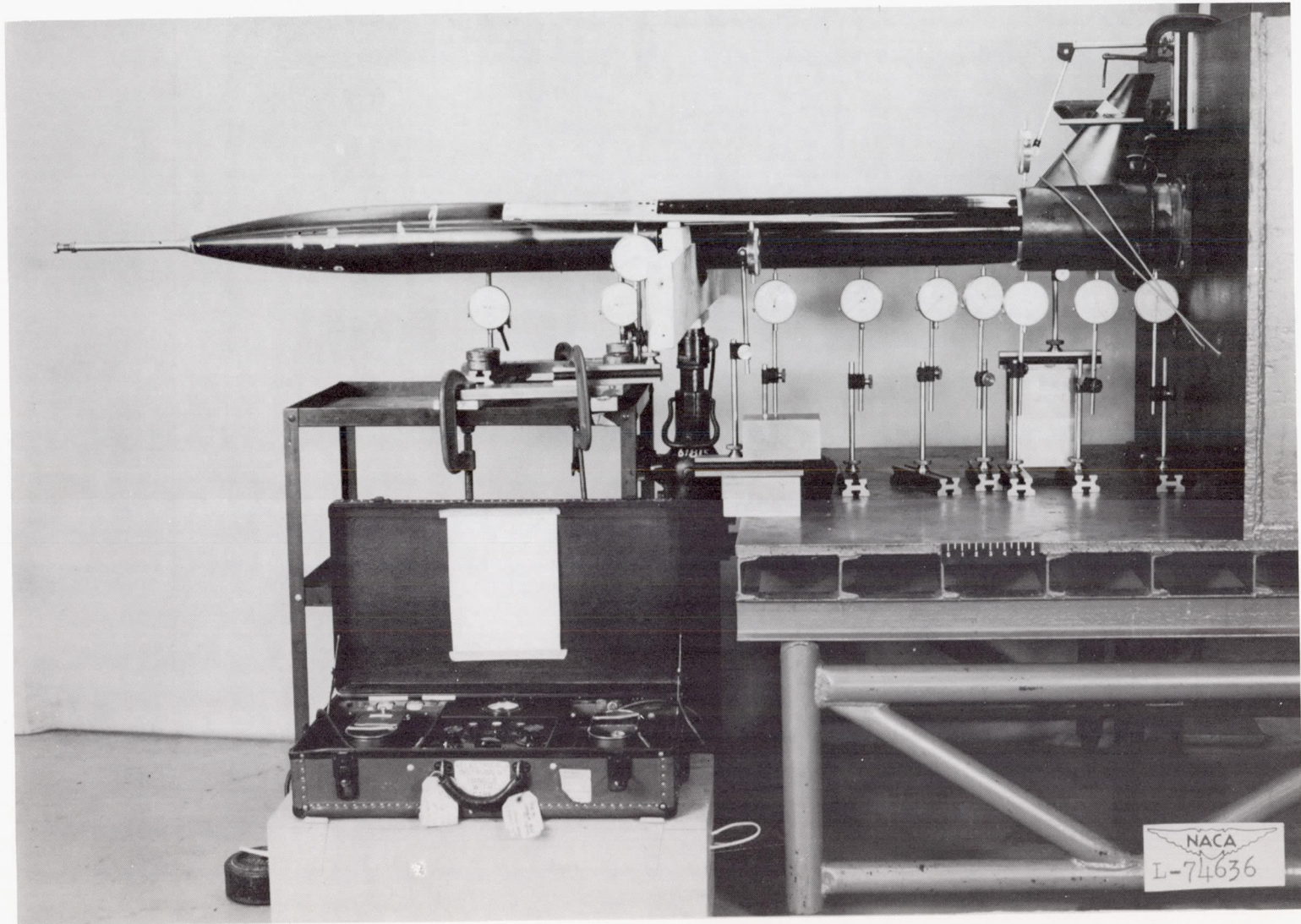
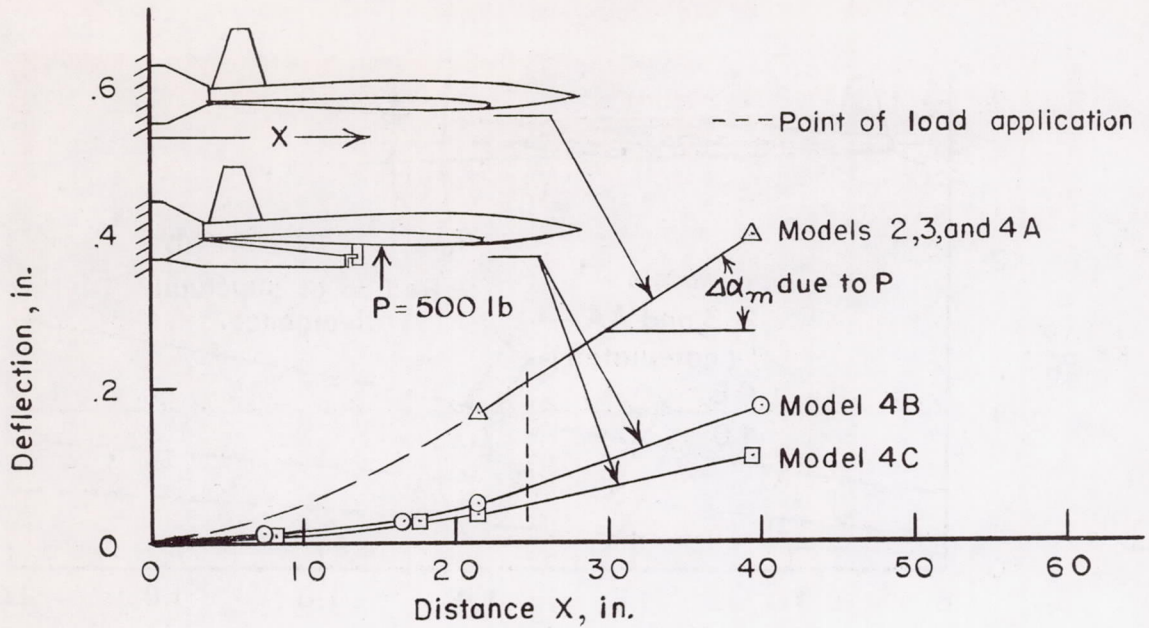
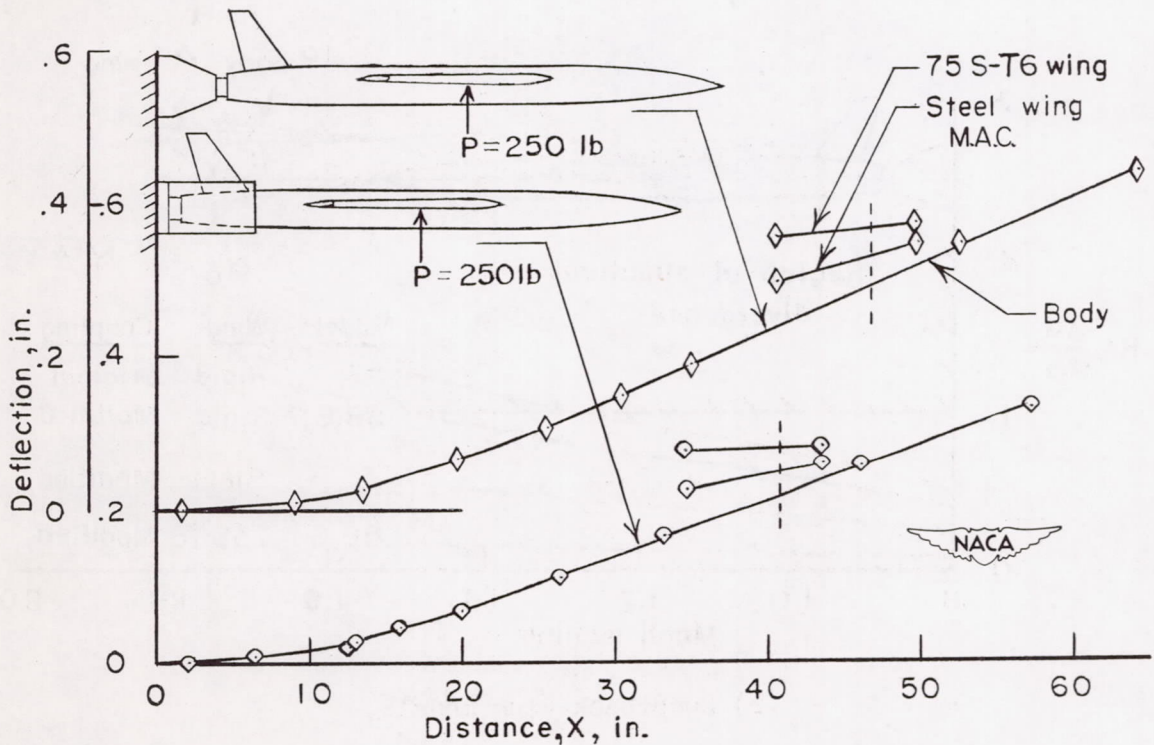


Figure 8.- Method of static testing a model mounted in its booster coupling.

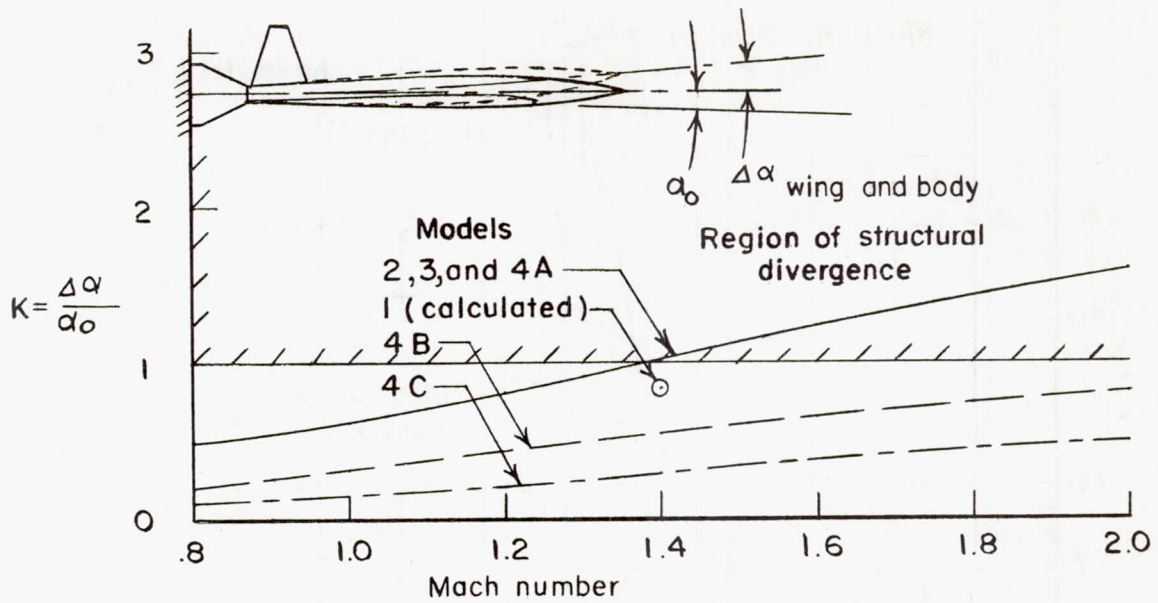


(a) Arrow-wing models.

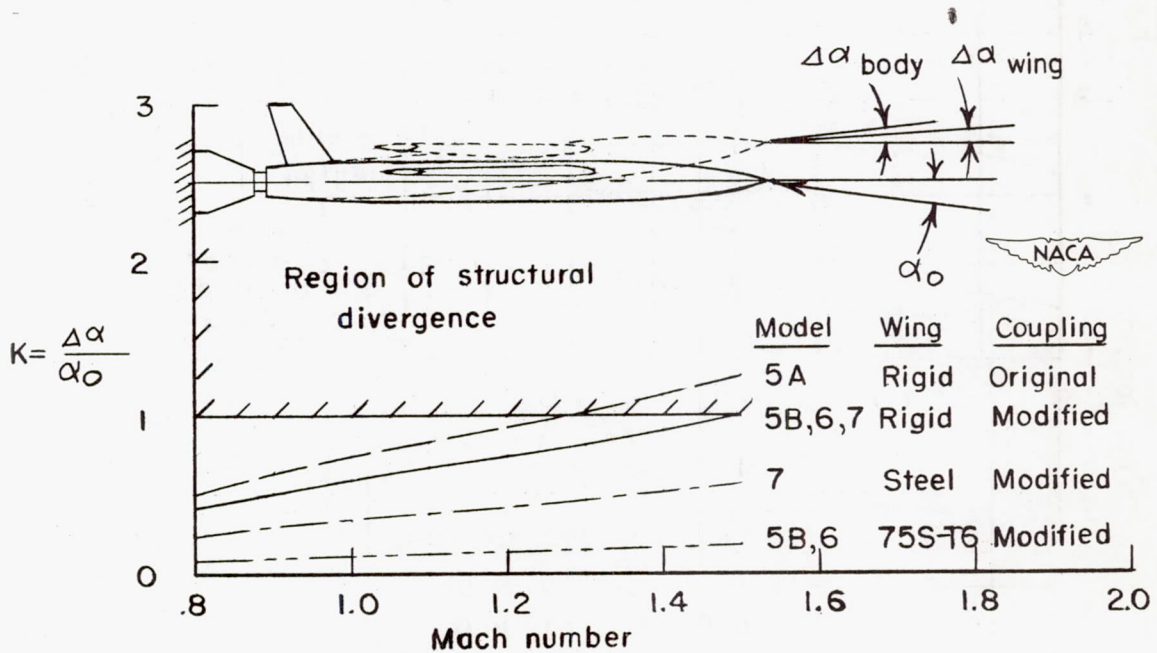


(b) Sweptback-wing models.

Figure 9.- Deflection data from static test of the arrow- and sweptback-wing models and booster couplings.

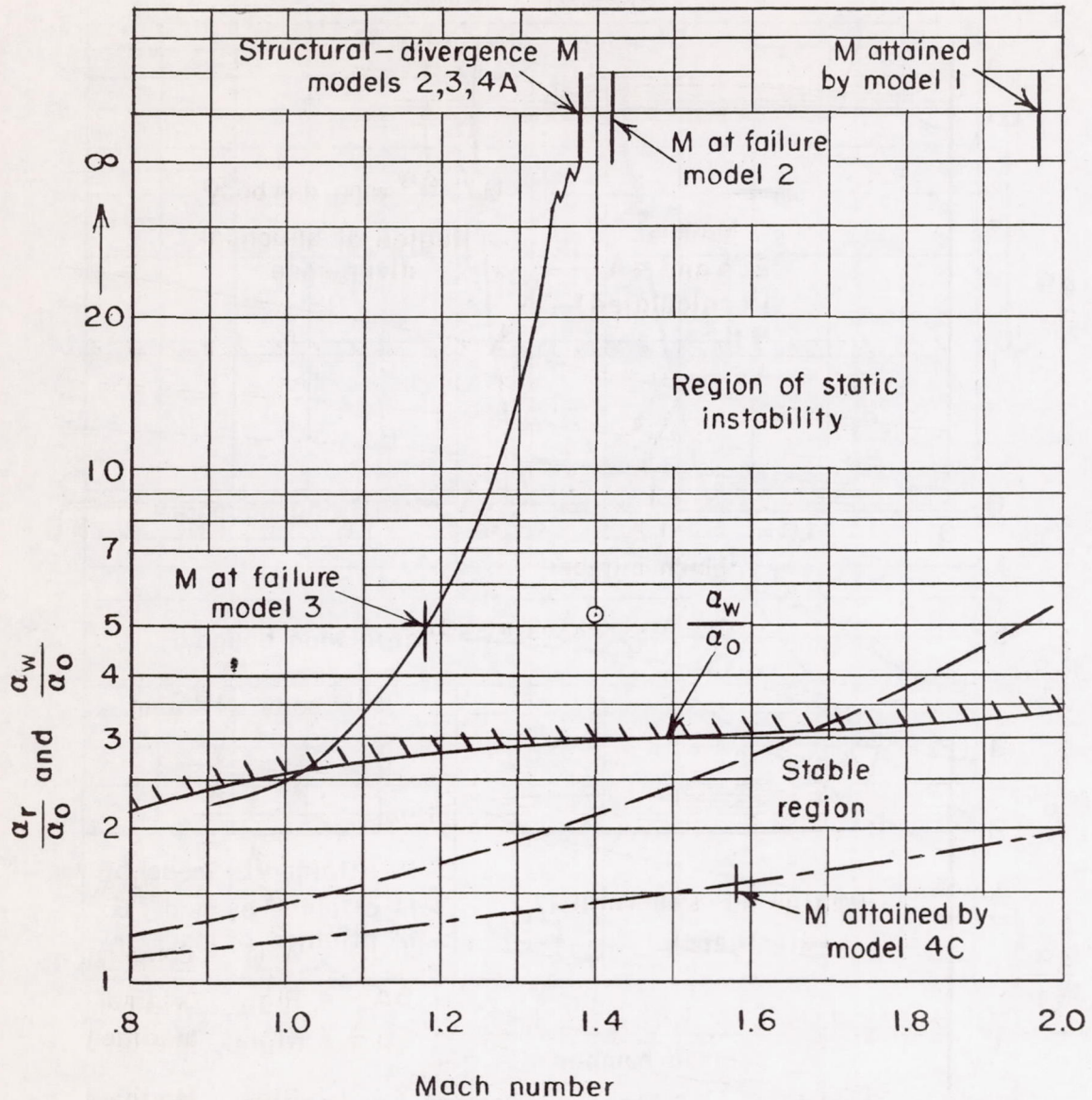


(a) Arrow-wing models.

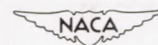


(b) Sweptback-wing models.

Figure 10.- Effect of Mach number on the initial incremental response factor K showing the beneficial effect of the modified couplings and of wing flexibility.

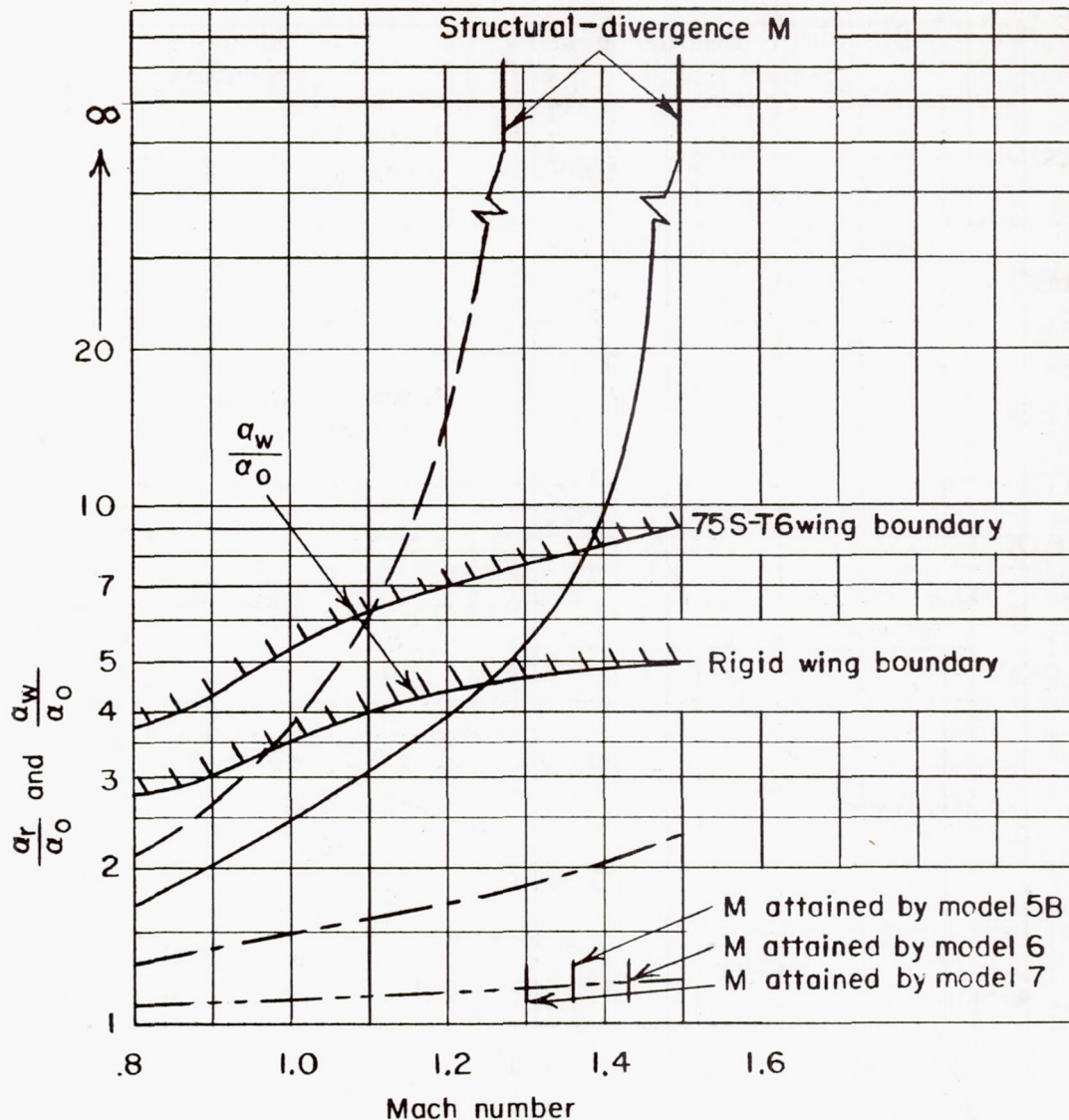


Curve	Models	Booster coupling
—————	2,3,4A	Original
⊙	1 (calculated)	Original
- - - - -	4B	Modified
- . - . -	4C	Modified and body reinforcement



(a) Arrow-wing models.

Figure 11.- Results obtained by the method of case II showing the variation with Mach number of the aeroelastic bending response for the models and of the static-stability boundary for the model-booster combinations.



Curve	Models	Wing	Booster coupling
— — —	5	Rigid	Original
— — —	5B,6,7	Rigid	Modified
— · — ·	7	Steel	Modified
— · — ·	5B,6	75S-T6	Modified

Static stability boundary.

Unstable

 stable



(b) Sweptback-wing models.

Figure 11.- Concluded.

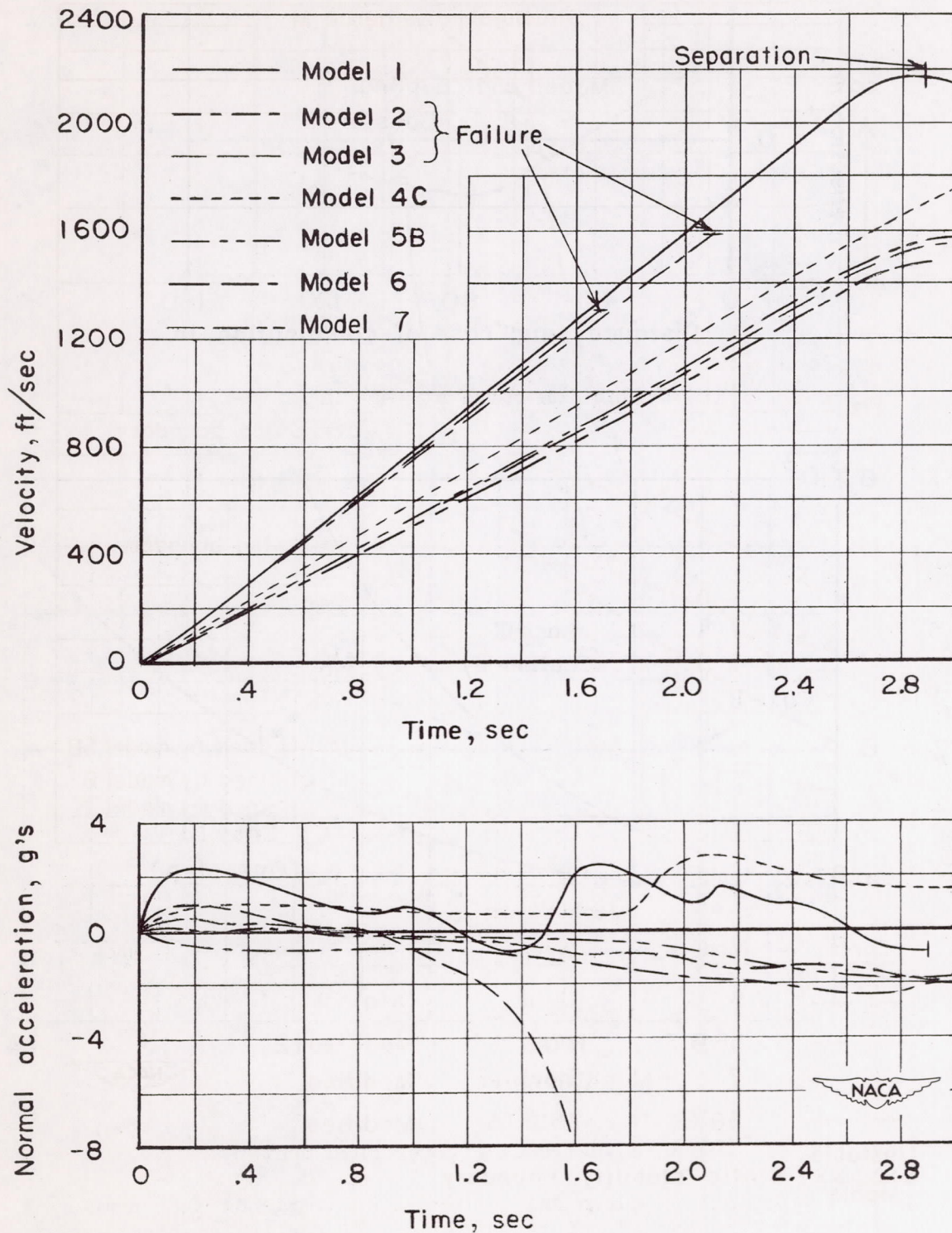
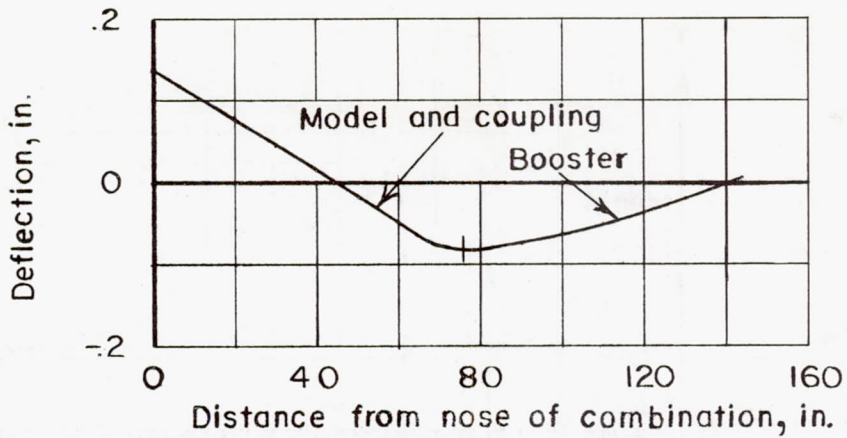
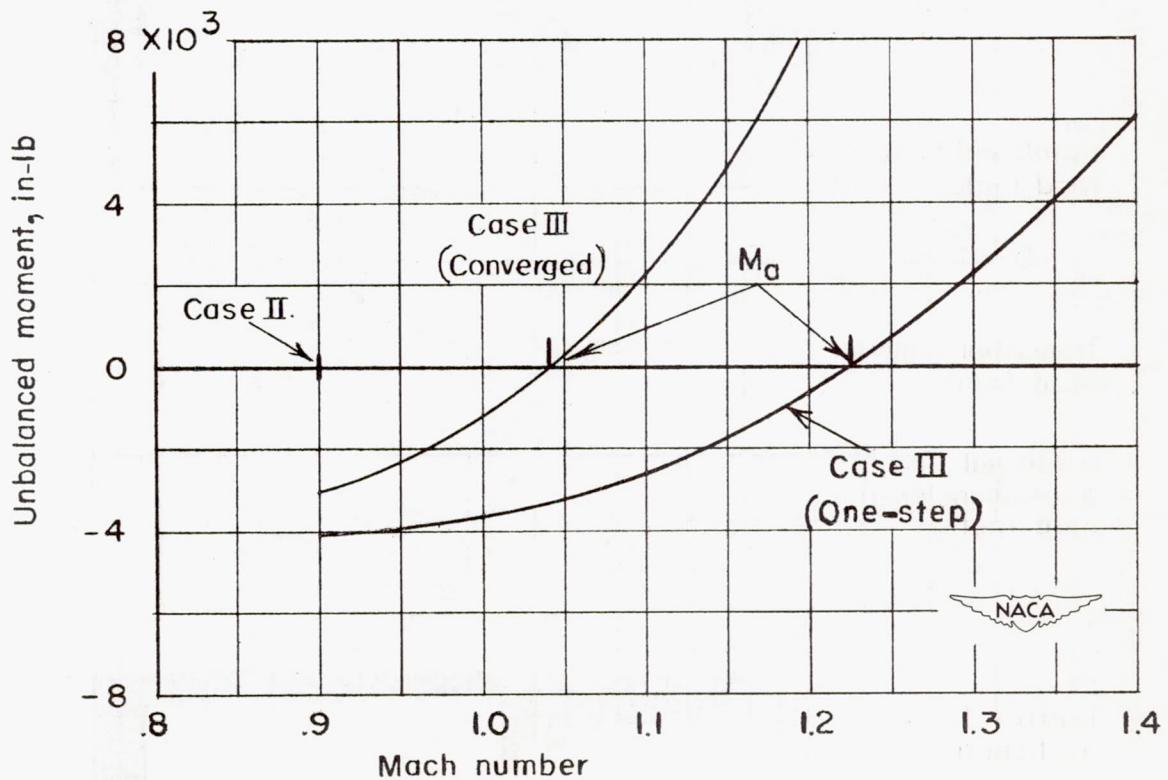


Figure 12.- Velocity and normal-acceleration time histories during boost.

(a) Deflection curve at $M = 0.9$.

(b) Aerodynamic-divergence Mach number.

Figure 13.- Deflection curve and aerodynamic-divergence Mach number as obtained by the methods of cases II and III for the combination of figure 5.

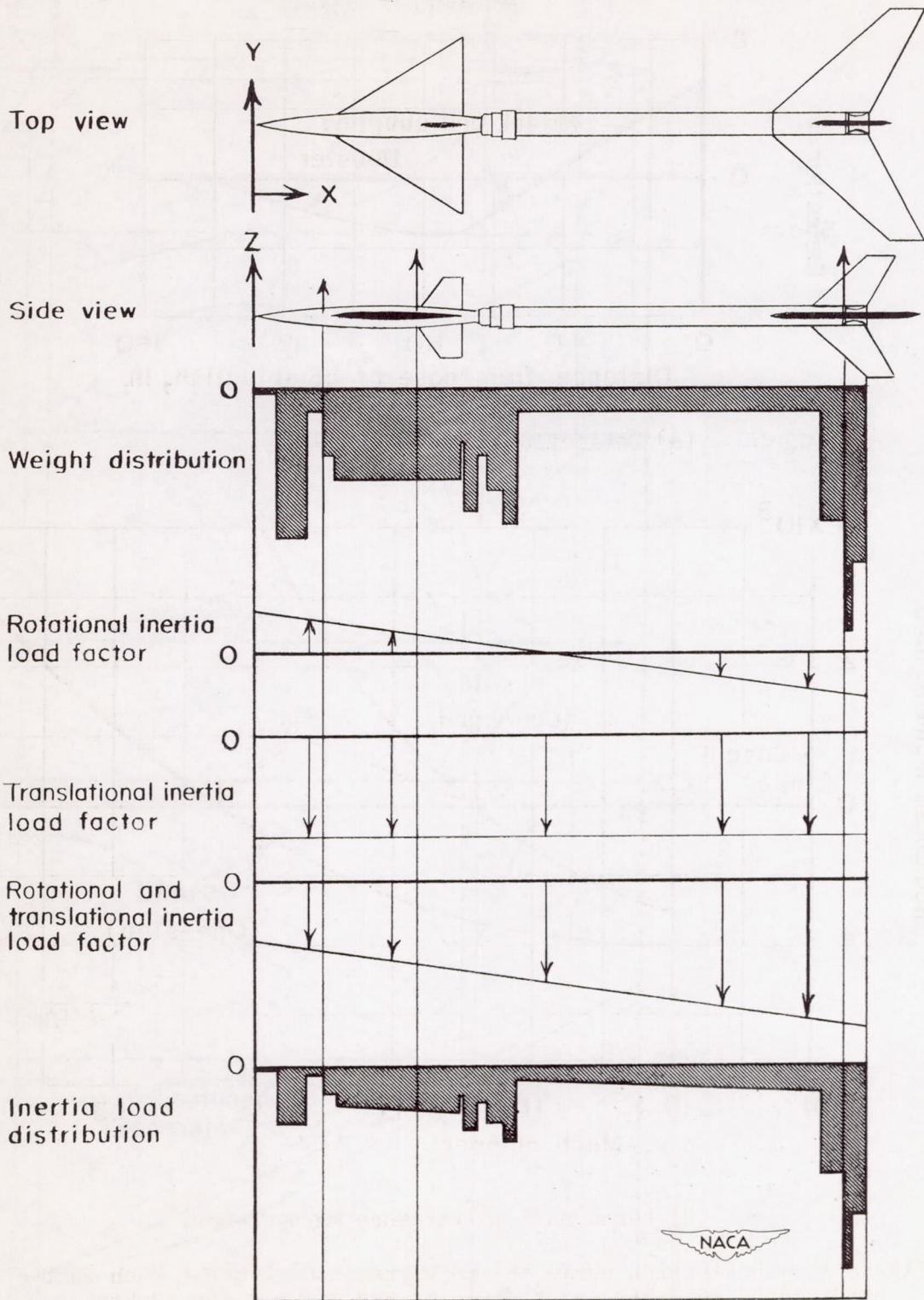


Figure 14.- Pictorial presentation of the method of obtaining the model-booster combination deflection curve for the method of case III.

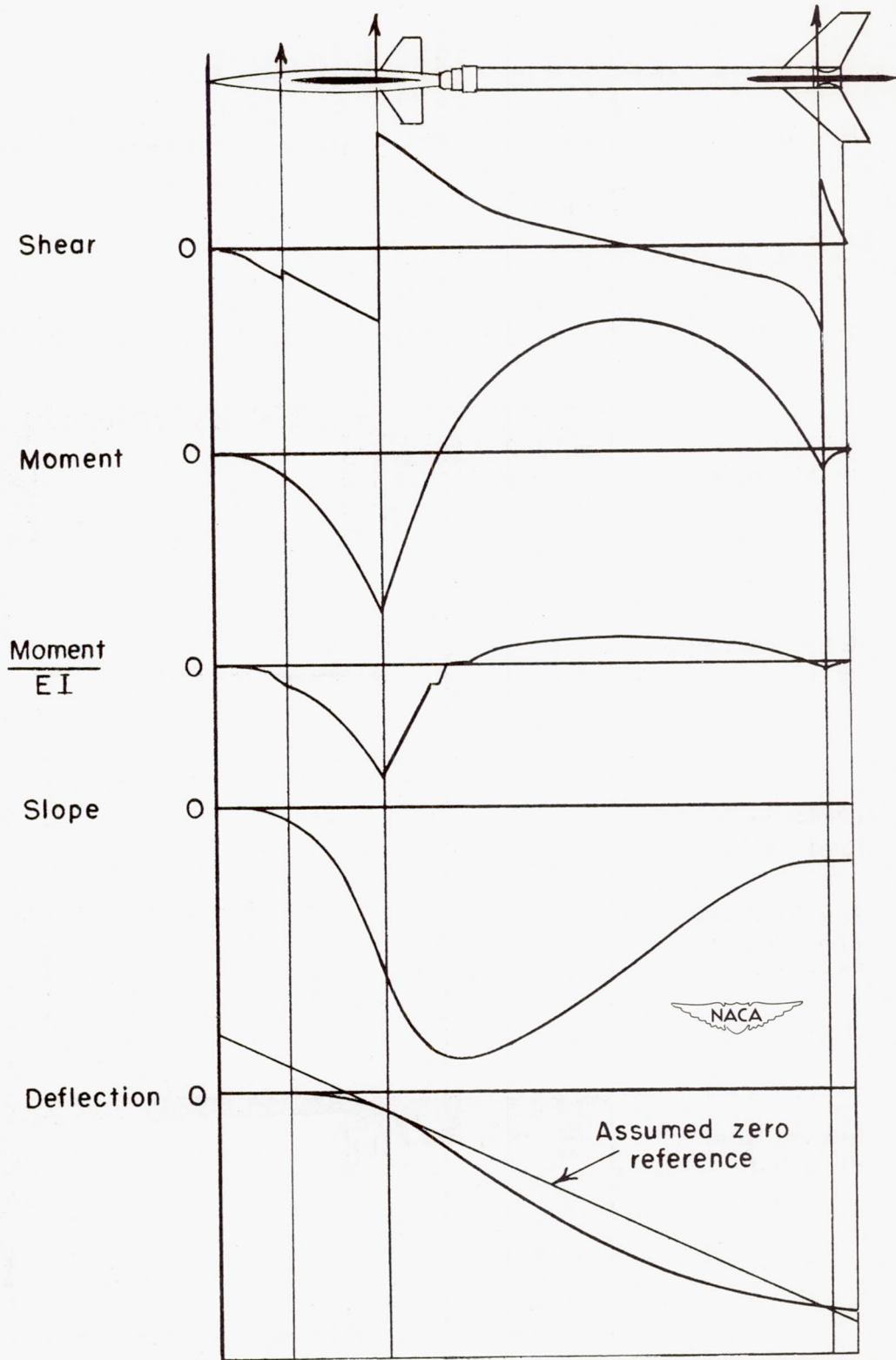


Figure 14.- Concluded.